BUCKLING ANALYSIS OF ELASTIC THIN SHELLS WITH STEPWISE VARIABLE THICKNESS UNDER STATIC THERMOMECHANICAL EFFECTS

O.P. Krivenko[1],
Candidate of Science (Engineering), Senior Researcher

P.P. Lizunov[1],
Doctor of Science (Engineering), Professor

O.B. Kalashnikov[2],
Candidate of Science (Engineering)

[1]*Kyiv National University of Construction and Architecture*
31, Povitryanykh Syl ave., Kyiv, Ukraine, 03037

[2]*State Scientific and Technical Center for Nuclear and Radiation Safety*
35-37 Vasyl Stus Street Kyiv, 03142

The presented results concern the study of nonlinear deformation, buckling, and natural vibrations of elastic shells with a nonuniform structure, with a particular focus on identifying bifurcation points in the pre-buckling domain.

Keywords: thin shell, geometrically nonlinear deformation, buckling, thermomechanical loading, bifurcation, universal three-dimensional finite element, moment finite element scheme.

Introduction. This paper is a continuation of the authors' systematic studies on the problems of nonlinear deformation, buckling, and natural vibrations of thin elastic shell structures of inhomogeneous composition under static thermomechanical loads [1–4]. The finite element method, on which the solution procedure for these classes of problems is based, can be confidently considered one of the most widely used numerical methods in structural mechanics [5–12].

In the developed method [1–4], an elastic inhomogeneous shell is treated as a three-dimensional body of small thickness without employing the conventional hypotheses of classical thin plate and shell theories [13–14]. The proposed approach to modeling elastic inhomogeneous shells, including shells with step-variable thickness, provides an efficient tool that allows one, within a unified methodology, to account for various realistic geometric features of structures. The shell may have ribs, channels, holes, sharp bends of the mid-surface, variable thickness, etc. For this purpose, a universal (within certain limits) three-dimensional finite element with additional variable parameters has been developed [1–4]. The finite element analysis is based on the geometrically nonlinear relations of the three-dimensional theory of thermoelasticity [15–17] and on the principles of the moment finite-element scheme (MFES) [6, 18–20]. Large displacements and small strains are considered, while the temperature field is assumed to be a known (prescribed) function of the coordinates and independent of the stress–strain state of the shell. In general, the behavior of a flexible elastic shell is a complex thermomechanical phenomenon. Different stages of loading can give rise to specific features in deformation and natural vibrations. In particular, in the pre-buckling domain, bifurcation points of equilibrium solutions may appear whose detection is an important step in studying buckling of shell structures. The developed buckling analysis method for inhomogeneous shells [1–4] makes it possible to detect the presence of bifurcation points and to trace new branches of solutions corresponding to alternative deformation modes. This is achieved by two approaches: (i) by the qualitative theory (in which case such points are determined within the accuracy of the load increment, i.e., within the interval of its variation), and (ii) by introducing a small imperfection into the initial mid-surface shape of the shell (which, in the pre-buckling domain, may transform a bifurcation point into a critical point). The capabilities of the proposed method are illustrated by the analysis of spherical axisymmetric panels of uniform thickness, for which the conditions of occurrence of asymmetric deformation and buckling modes along with symmetric ones were determined [4]. A classical benchmark problem [21,

22] was considered, namely, the determination of the critical load for panels of different curvatures rigidly clamped along the contour and subjected to a uniform pressure of intensity q. The effectiveness of the developed approach has been confirmed.

1 Objective of the study. This paper continues the research presented in [4]. The results of the analysis of the deformation and buckling behavior of elastic shells are presented. Among all the studies conducted by the authors [1–4], this work focuses primarily on shells for which the «load–deflection» curves ($\bar{q} - \bar{u}$) exhibit bifurcation points in the pre-buckling deformation domain. Both constant-thickness and stepwise variable-thickness shells are considered. The results are presented on the influence of both structural parameters of the shells and thermomechanical loading on the buckling behavior of inhomogeneous elastic shells.

The results are presented in terms of the dimensionless parameters for the load $\bar{q} = a^4 q / (Eh^4)$ and the deflection $\bar{u}^{1'} = u^{1'}/h$ along the Cartesian axis $x^{1'}$. Here a is the characteristic in-plane dimension of the panel, h − is the thickness, and E − is the elastic modulus. For convenience, the figures include corresponding notations indicating the class of problems being considered.

2 Buckling and natural vibrations of a constant-thickness panel. A square smooth spherical panel is considered (Fig. 1). The panel is simply supported along its contour and subjected to a uniform pressure. The shell material is isotropic. The curvature of the panel is defined by the parameter $K = 2a^2/(Rh)$, where R − radius of the mid-surface of the panel. The input data are as follows: $E = 2{,}1 \cdot 10^6$ kg/cm², Poisson's ratio $\nu = 0{,}3$ and density $\rho = 7.85 \cdot 10^{-3}$ kg/cm³.

2.1 The behavior of a *shallow spherical panel* with the curvature parameter $K = 32$, $h = 1$ cm, $a = 60h$, $R = 225h$ is investigated.

A detailed analysis of the buckling of the panel according to the static criterion, where the solution is presented as the $\bar{q} - \bar{u}$ curve, is given in [1]. In [2], the results of the modal analysis of this panel are presented. The issue of the validity of employing symmetry planes in the finite-element shell model (FESM) was studied. Naturally, the use of symmetry planes simplifies the formulation of the buckling problem and makes the solution process more manageable; however, it simultaneously eliminates the possibility of the occurrence of skew-symmetric vibration modes, special points, and bifurcated branches of nonlinear solutions. Figure 2 shows the «load–frequency» curves ($\bar{q} - \omega_i$) corresponding to two formulations of the problem: the entire panel without symmetry planes, frequencies ω_i; and a quarter panel with the FESM including two symmetry planes, frequencies $\tilde{\omega}_i$. The corresponding vibration modes of the panel at the initial loading stage ($\bar{q} = 0$) are presented in Table 1. In the last column of the table schematic representations of the natural vibration modes are provided.
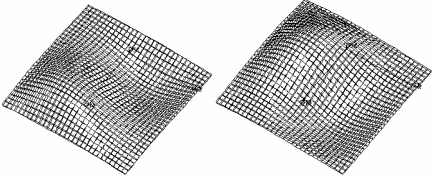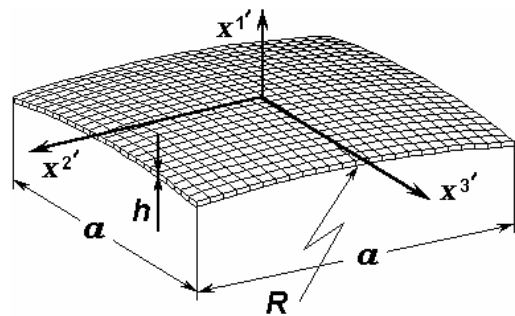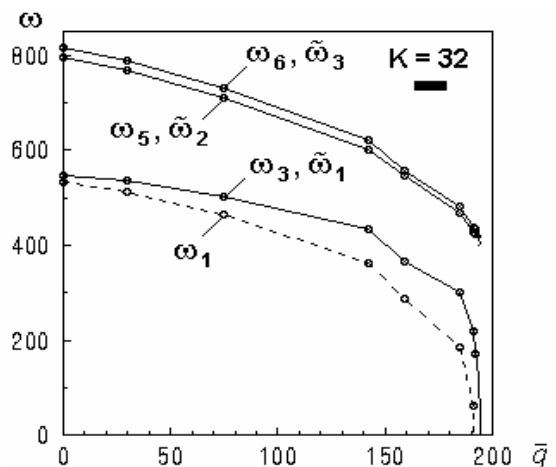

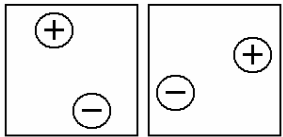Fig. 1. Shallow spherical panel of constant thickness

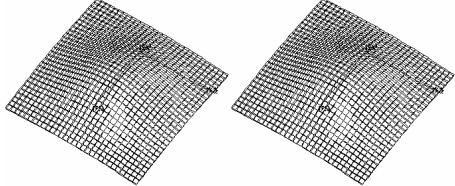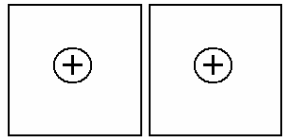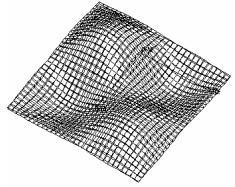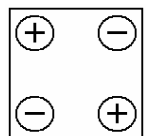Fig. 2. Natural vibration frequencies for the finite-element model of the entire panel (ω) and the quarter panel ($\tilde{\omega}$)

Table 1

ω, Hz	$\bar{q} = 0$		
$\omega_1 = \omega_2 = 533{,}78$			
$\omega_3 = \widetilde{\omega}_1 = 547{,}40$			
$\omega_4 = 691{,}24$			

The FESM with two symmetry planes excludes asymmetric vibration modes. The frequencies corresponding to the symmetric vibration modes are identical for both FESM model variants. It should be noted that when considering the FESM with a single symmetry plane (half of the panel), the conjugated vibration modes corresponding to multiple frequencies are eliminated. For example, in our case, the frequency ω_2 and the associated vibration mode are disregarded (Table 1). Therefore, a complete buckling analysis of shells combined with modal analysis should be carried out using a FESM without symmetry planes. The FESM with one symmetry plane may also be used; however, in this case, one should consider the possible exclusion of multiple eigenfrequencies.

Considering the deformed state of the shell while ignoring the stresses accumulated at the load increment steps (prestress) leads to an incorrect calculation of frequencies (solid curve) and a false determination of the upper critical load q_{cr}^{up} by the dynamic criterion (Fig. 3). The dashed curve $\bar{q} - \omega$ corresponds to the calculation with prestress considered at each load step. Circles indicate the load levels at which the modal analysis was performed.

Fig. 3. Comparison of the results with (dashed curve) and without (solid curve) consideration of the pre-stressed state

The algorithm for solving the problem of nonlinear deformation and buckling of the shell makes it possible to identify bifurcation points on the $\bar{q} - \bar{u}$ curve. For this purpose, the qualitative theory is applied. The occurrence of bifurcation points ($*$) is associated with the appearance of closely spaced equilibrium states of the shell. From the mathematical point of view, such a point is characterized by the degeneration of the determinant of the linearized stiffness matrix of the governing system of equations, i.e., the first approach (i) [1, 4] is used. The stress–strain state of the shell in the vicinity of the bifurcation point (at the load level $\bar{q}*$) changes smoothly. This
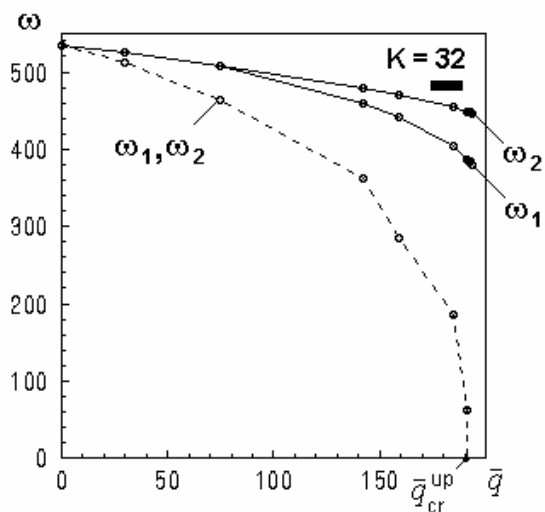
process corresponds to a small deflection buckling. The load value $\bar{q}*$ corresponding to the first bifurcation point may be taken as the critical one.

For the shallow spherical panel $K = 32$, the $\bar{q} - \bar{u}$ curve has a simple form (Fig. 4, a) and can be described as a *oabc* curve. In the pre-buckling domain, using approach (i), at $\bar{q}^{*i} = 191.6$ a possible bifurcation point was detected. To determine this point (value $\bar{q}*$) more precisely, according to approach (ii), a small asymmetric perturbation $\eta \sin(2\pi\xi)$ ($\xi = x/a$ – dimensionless in-plane coordinate) is introduced into the initial mid-surface geometry of the panel, which can be interpreted as an initial imperfection of the shell shape. The perturbation parameter was taken as $\eta = 0,01$.

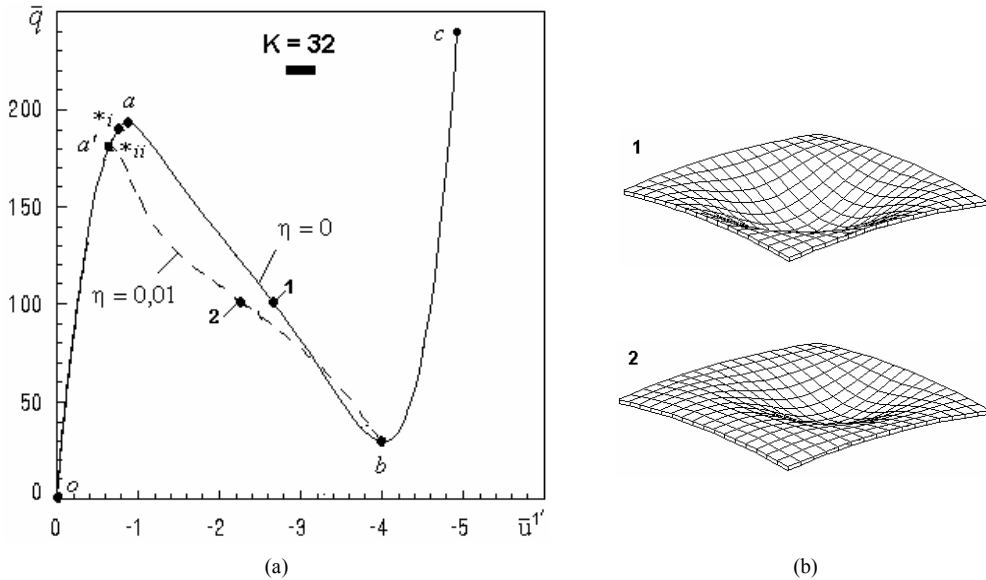(a)   (b)

Fig. 4. Identification of the bifurcation point for a shallow square spherical panel and the corresponding deformation modes

The introduction of a small shape perturbation transforms the bifurcation point into a critical one. The resulting new $\bar{q} - \bar{u}$ curve acquires the form *oa'bc* ($\eta = 0,01$) in contrast to the curve *oabc* ($\eta = 0$) for the perfect panel. In the *a'b* range, this curve is shown by the dashed line. The obtained value $\bar{q}* = \bar{q}^{*ii} = 182,1$ ($\eta = 0,01$) is 6% lower than the upper critical load $q_{cr}^{up} = 193,7$ ($\eta = 0$) of the perfect panel. Equilibrium post-buckling deformation shapes are shown in Figure 4, b: an axisymmetric deformation shape at point 1 in the *ac* range for the panel of ideal shape, and a skew-symmetric deformation shape at point 2 in the *a'c* range for the perturbed panel.

A small perturbation of the initial shell shape affects its natural frequencies. A divergence of the $\bar{q} - \omega_1$ curves is observed as the load approaches to q_{cr}^{up} (Fig. 5). Starting from the load $\bar{q} = 142$, the $\bar{q} - \omega_1$ curves corresponding to the perfect ($\eta = 0$) and imperfect ($\eta = 0,01$) shell shapes begin to deviate. The load at which $\omega_1 = 0$ is taken as the upper critical load according to the dynamic buckling criterion [23].

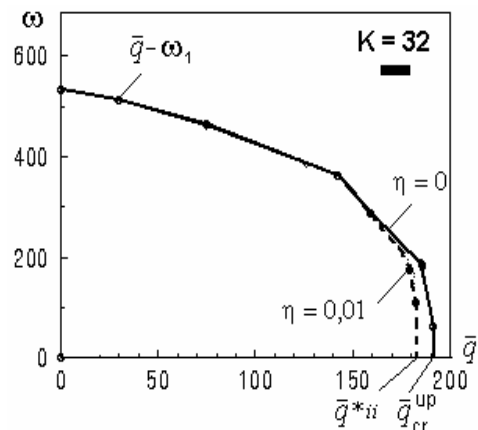For the panel with an ideal middle surface, according to the dynamic criterion $\bar{q}* = \bar{q}_{cr}^{up} = 191,8$

Fig. 5. The $\bar{q} - \omega_1$ curves for a shallow panel of constant thickness, *K*=32

(Fig. 5). The difference from the critical load determined by the static criterion is less than 1%.

For the panel with a perturbed middle surface (approach (ii)), according to the dynamic criterion, $\overline{q}^{*ii} = \overline{q}_{cr}^{up} = 183,0$ (Fig. 5). The difference from $\overline{q}^{*i} = 182,1$, obtained using approach (i), is less than 0,5%.

The obtained results confirm the effectiveness of applying a comprehensive approach to the analysis of shell buckling.

2.2 The behavior of a *smooth shallow shell* of constant thickness with a curvature parameter $K = 64$ and $h = 1$ cm, $a = 120h$, $R = 450h$ is studied.

In the pre-buckling and post-buckling domain, the «load – deflection» curves for this shallow panel exhibit a complex shape (Fig. 6 (a), (b)). The curves $\overline{q} - \overline{u}$ are presented for characteristic points o (panel center) and b (quarter panel center). Unlike the shallow panel, the buckling of the shallow shell occurs in two stages. In the first stage, the deflection sharply increases in the panel at the middle of the quarters, points b. At the same time, the panel center practically does not deform. This corresponds to a local buckling, with the formation of two stiffening ridges along the symmetry axes of the panel (Fig. 6, c). On the curves $\overline{q} - \overline{u}$ this moment of deformation corresponds to poin 1, which has the following characteristics: load $\overline{q} = 777.7$, deflection at point o $\overline{u}_o^{1'} = -0.1445$, deflection at points b $\overline{u}_b^{1'} = -0.6677$. For clarity, the shapes are shown in an enlarged scale in the Figure.
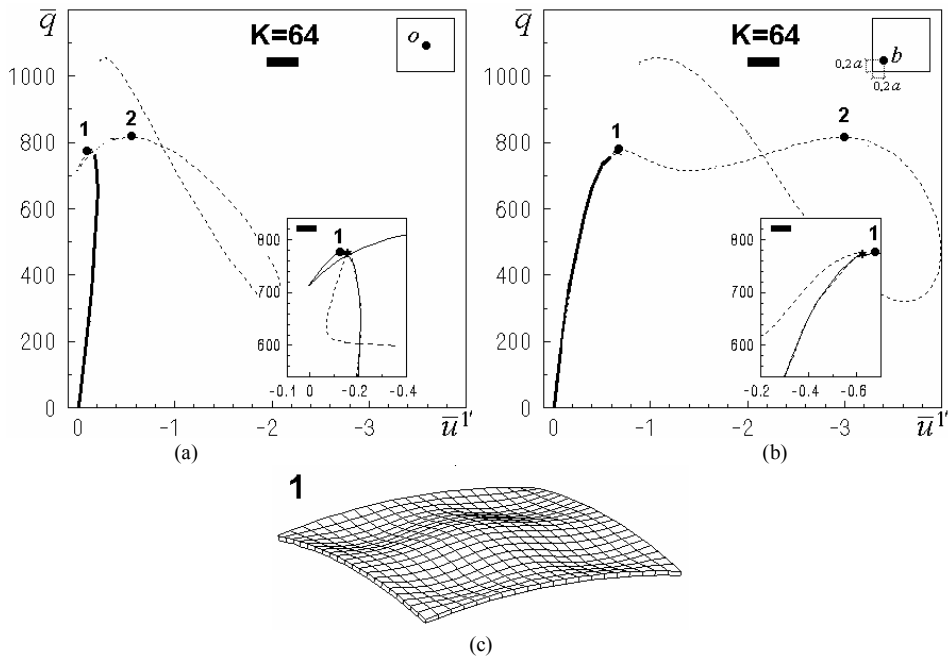

Fig. 6. A shallow panel of constant thickness (K=64): the $\overline{q} - \overline{u}$ curves at points o (a) and b (b); deformed shape (c)

At the second stage, a global buckling of the panel occurs (point 2) accompanied by a pronounced snap-through across the entire shell surface: the load is $\overline{q} = 815$, and the deflections at points o and b are $\overline{u}_o^{1'} = -0.5500$ and $\overline{u}_b^{1'} = 2.999$, respectively. The deformation shapes in the pre-buckling and post-buckling domains are similar.

In the pre-buckling domain, when approaching point 1 at a load of $\overline{q}^{*i} = 173.5$ according to approach (i), a possible bifurcation point $*$ was detected. The existence of this point is also confirmed by the analysis performed using the LIRA-SAPR [24]. The computational process in the LIRA-SAPR stopped precisely at this point. A comparison with the results obtained using the LIRA-SAPR showed a complete agreement of the $\overline{q} - \overline{u}$ curves in the pre-buckling domain (bold line).

According to approach (ii), the introduction of a small asymmetric perturbation into the ideal midsurface geometry of the shell made it possible to more accurately determine the bifurcation point $*$ ($\overline{q}^{*ii} = 775.6 < \overline{q}_{cr}^{up}$) and to trace the branching curve from this point (dash-dotted line, Fig. 6).

The loading process of the considered non-shallow panel is accompanied by a rearrangement of vibration modes. On the $\overline{q} - \omega_1$ curves (Fig. 7), circles indicate the loading moments at which a change in the character of the panel's natural vibration modes occurs (Fig. 8). This transformation of vibration modes depends on the change in the multiplicity of frequencies during loading. In the initial unloaded state ($\overline{q}^{i=0}$), the frequencies $\omega_1 = \omega_2$ are multiple. At loads $\overline{q}^{i=7}$, the frequencies $\omega_3 = \omega_4$ become multiple, and at loads $\overline{q}^{i=9}$, the frequencies $\omega_2 = \omega_3$ become multiple. The

Fig. 7. The $\overline{q} - \omega_1$ curves for a non-shallow panel of constant thickness, $K=64$

rearrangement of vibration modes takes place at loads $\overline{q}^{i=7}$ and $\overline{q}^{i=9}$. For the frequencies obtained at each loading step, their variation spectrum is quite dense.
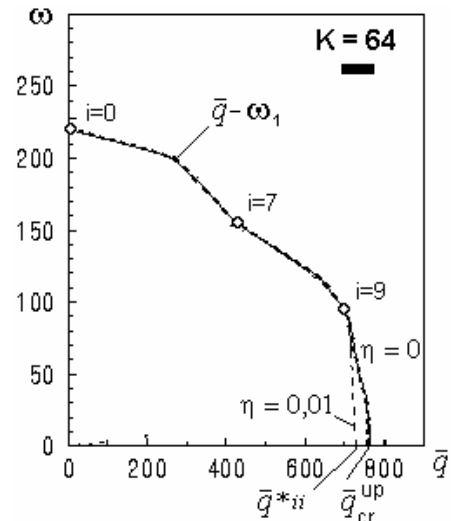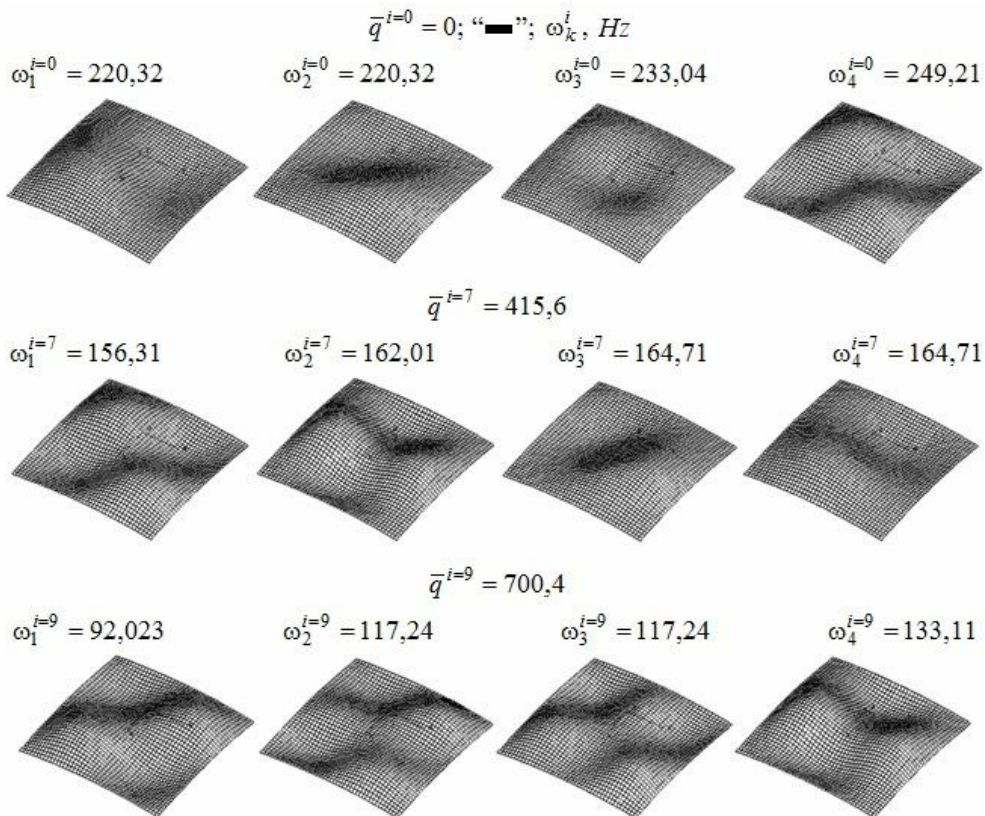

Fig. 8. Transformation of vibration modes of a non-shallow panel of constant thickness, $K=64$

Comparing the behavior of shallow ($K=32$) and non-shallow ($K=64$) panels, it can be noted that for the non-shallow panel the $\overline{q} - \overline{u}$ curves are more complex. Buckling of the non-shallow panel occurs in two

stages, with the maximum deformation developing not at the center, as in the shallow panel, but in the middle of its quarters. The loading process is accompanied by a transformation of the vibration modes.

3 Buckling and natural vibrations of a ribbed panel. The behavior of a ribbed non-shallow panel is studied (K=64, h =1 cm, a=120h, R=450h). The concave side of the shell is reinforced with a pair of central crossing ribs: $h_r = 2h$ is a rib height excluding the shell thickness h, $b_r = 2h$ is a rib width.

The deformation pattern of this ribbed panel (Fig. 9) differs only slightly from that of the previously considered non-shallow shell without ribs. This is due to the ribs being in areas where natural stiffness ridges form during the deformation of the smooth shell (Fig. 6 (c)).
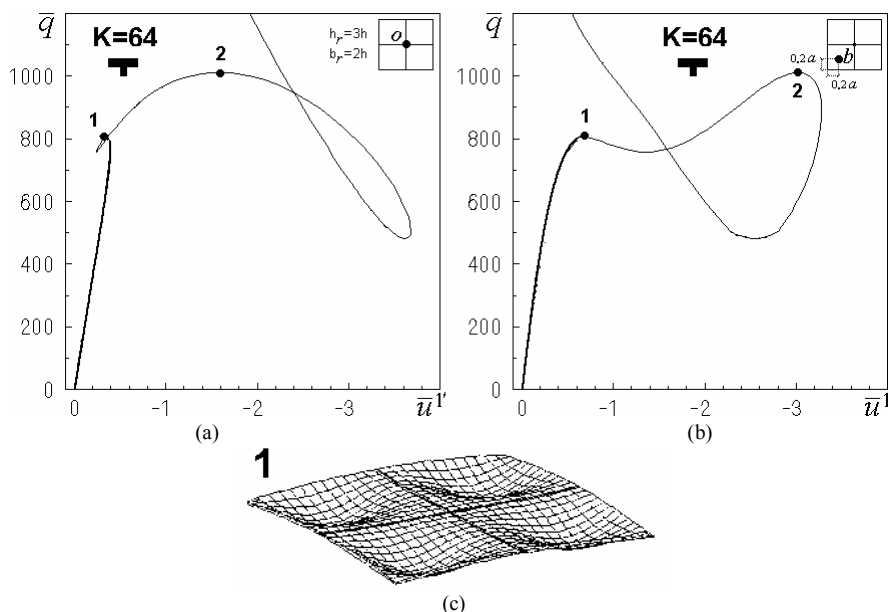

Fig. 9. Non-shallow ribbed panel (K=64): the $\bar{q}-\bar{u}$ curves at points o (a) and b (b); deformation shape (c)

The presence of the central rib pair has almost no effect on the magnitude of the critical load, which increased only by 3,3%, compared to the smooth shell. 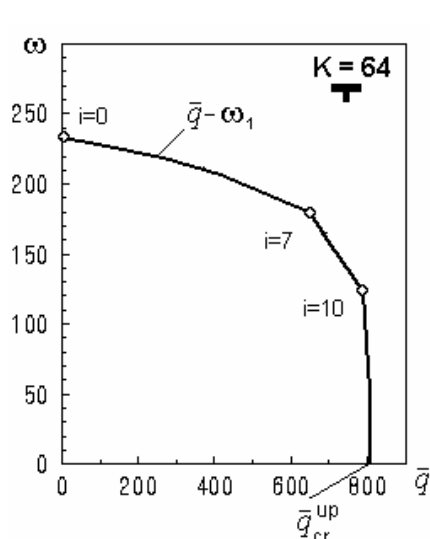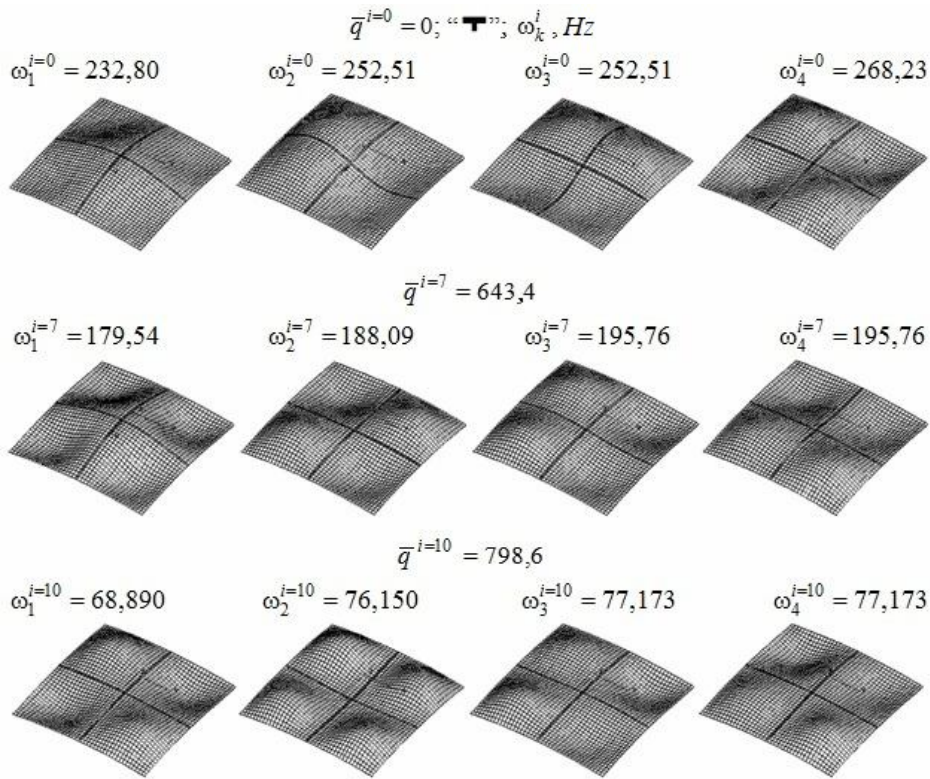The $\bar{q}-\bar{u}$ curve at the characteristic point 1 shows the following values: $\bar{q} = 804,4$, $\bar{u}_o^{1'} = -0,3470$, $\bar{u}_b^{1'} = -0,7087$. The overall buckling of the panel (point 2) occurs at a load of $\bar{q} = 1012$.

In the pre-buckling deformation domain for the considered ribbed panel, a bifurcation point ($\bar{q}^{*i}$ =800,2), is also observed, identified according to approach (i). Comparison with results obtained using the LIRA-SAPR (bold curve) shows complete agreement of the curves $\bar{q}-\bar{u}$ in this domain.

The $\bar{q}-\omega_1$ curve (Fig. 10), similar to the smooth panel, exhibits a mode shape transformation (Fig. 11). The loads at which this transformation occur are marked with circles. For the ribbed panel, at loads $\bar{q}^{i=0} \le \bar{q} < \bar{q}^{i=7}$, the frequencies $\omega_2 = \omega_3$ are multiples; at loads $\bar{q}^{i=7} \ge \bar{q}$, the frequencies $\omega_3 = \omega_4$ become multiples. The mode shape transformation occurs at loads $\bar{q}^{i=7}$ and $\bar{q}^{i=10}$.

Fig. 10. The $\bar{q}-\omega_1$ curve for the non-shallow ribbed panel, K=64

$$\overline{q}^{i=0} = 0; \quad \text{“} \blacktriangledown \text{”}; \quad \omega_k^i, Hz$$

$\omega_1^{i=0} = 232,80$ $\omega_2^{i=0} = 252,51$ $\omega_3^{i=0} = 252,51$ $\omega_4^{i=0} = 268,23$

$$\overline{q}^{i=7} = 643,4$$

$\omega_1^{i=7} = 179,54$ $\omega_2^{i=7} = 188,09$ $\omega_3^{i=7} = 195,76$ $\omega_4^{i=7} = 195,76$

$$\overline{q}^{i=10} = 798,6$$

$\omega_1^{i=10} = 68,890$ $\omega_2^{i=10} = 76,150$ $\omega_3^{i=10} = 77,173$ $\omega_4^{i=10} = 77,173$

Fig. 11. Mode shape transformation of the non-shallow ribbed panel, $K=64$

It can be concluded that the behavior of smooth and ribbed shallow panels $K=64$ remains similar. This is explained by the fact that the installed cross ribs pass through the natural stiffness ridges inherent in the smooth shell during deformation, which enhances the local rigidity of the structure. The conducted study confirmed the effectiveness of the applied method for analyzing ribbed shells.

4 Buckling of a panel with channels. A smooth shallow panel ($K=32$, $h=1$ cm, $a=60h$, $R=225h$) weakened by four cross channels is considered. The channels are symmetrically arranged on the inner and outer surfaces of the panel (Fig. 12) and have identical dimensions: length a, width $b_c = 6h$, depth $h_c = 0,7h$.

The obtained $\overline{q} - \overline{u}$ curves are plotted for the deflections at two characteristic points of the shell: o is the panel center, b is the intersection point of the channels (Fig. 13 (a)). A comparison of the results obtained using the MFES and LIRA-SAPR (bold curve) and SCAD [25] (dashed curve), shows that the curves fully coincide in the pre-buckling domain. The analysis in LIRA-SAPR terminated at the bifurcation point (marked with '*' on the graph), which the program interprets as the upper critical load. The bifurcation point was also detected in the calculations performed by the MFES (approach (i)). To refine the value of $\overline{q}^{*i}$ approach (ii) was applied, which involves introducing a small asymmetric perturbation ($\eta = 0,01$) into the initial mid-surface shape of the shell. The calculation results are given in Table 2. The branching of the new equilibrium path is shown by the dash-dot curve.

It should be noted that the deformation shapes of the shell obtained using different algorithms (MFES, LIRA-SAPR, and SCAD) agree well with each other (Fig. 13 (b)). At the moment of buckling, the deflection at the panel center is smaller than in the region of the channel.
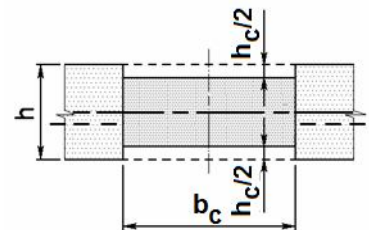
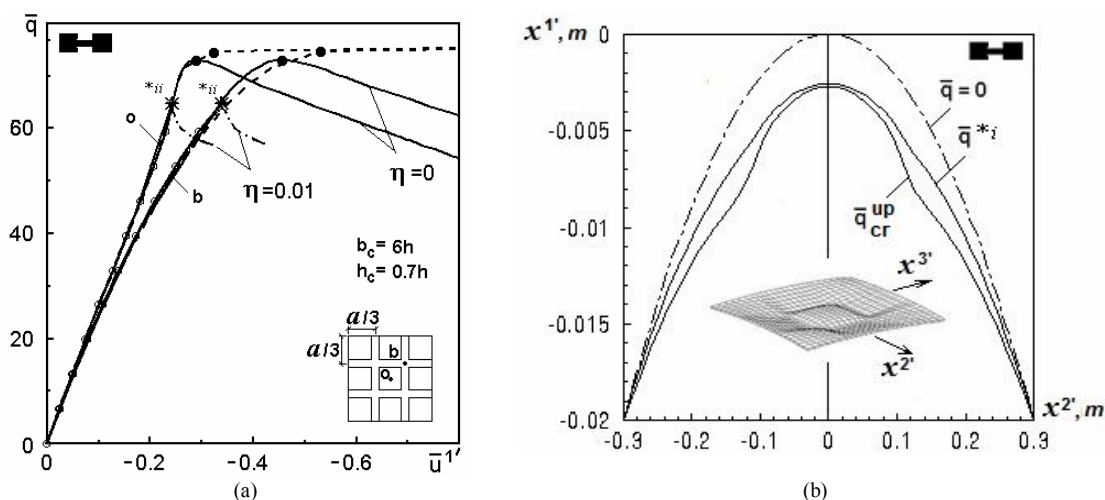Fig. 12. Schematic representation of a shell segment with channels, ▄▬

Fig. 13. Spherical panel with channels (K=32): the $\overline{q}-\overline{u}$ curves (a) and
deformation shapes of the shell at characteristic load levels (b)

Table 2

Method of Analysis	$\overline{q}_{cr}^{up}/\overline{u}_{cr}^{1'up}(o)$	$\Delta^q/\Delta^u,\%$	$\overline{q}^{*ii}/\overline{u}^{1*ii}$	$\Delta^{q*ii}/\Delta^{u*ii},\%$
MFES	72,94/−0,2876	0/0	63,34/−0,2410	0/0
LIRA-SAPR	—	—	64,79/−0,2451	2,89/1,70
SCAD	74,71/−0,3289	2,43/12,81	—	—

It is shown that the developed method is effective for studying nonlinear deformation, buckling, and post-buckling behavior not only of smooth shells of constant thickness and ribbed shells, but also in analyzing the behavior of shells with structural weakenings, such as channels.

5 Effect of preliminary heating on buckling of a thin shell. A shallow axisymmetric spherical panel of constant thickness is considered. The panel is subjected to a temperature field and an external uniform pressure. The shell is hinged along its contour ($\overset{\approx}{\mathbb{N}}$). The input data are as follows: $k = H/h$ is a parameter, characterizing the shallowness of the axisymmetric panel, $H=4h$ is the rise of the panel, $h=1$ cm, $a=100h$, $\alpha = 0.125\cdot10^{-4}$ grad^{-1} is the coefficient of linear thermal expansion.

In the calculations, the effect of heating and pressure on the shell is treated as a combined thermomechanical loading process carried out in two stages. First, the panel is heated to a specified temperature: $T=0,+20,+40^{\circ}$C. This causes nonlinear deformation of the shell. The heating acts as a preliminary disturbance of the panel's stress–strain state during subsequent loading by a uniformly distributed normal pressure of intensity q. The additional loading by pressure is applied while maintaining a fixed temperature field T.

The evolution of the $\overline{q}-\overline{u}$ curves of the spherical panel depending on the amount of preliminary heating is shown in Fig. 14. In the absence of heating ($T = 0^{\circ}$C) and when the panel is heated to $T = 20^{\circ}$C, the curves $\overline{q}-\overline{u}$ have a rather complex shape. In the domain of the upper critical load $\overline{q}_{cr}^{up}$, loops appear and bifurcation points ($\overline{q}* < \overline{q}_{cr}^{up}$) are observed. The introduction of an asymmetric disturbance into the mid-surface of the shell according to approach (ii) ($\eta = 0.001$) made it possible to obtain a new branch of the solution (dash-dotted curve). In the vicinity of this point, the axisymmetric deformation mode of the shell transitions into an adjacent non-axisymmetric one.
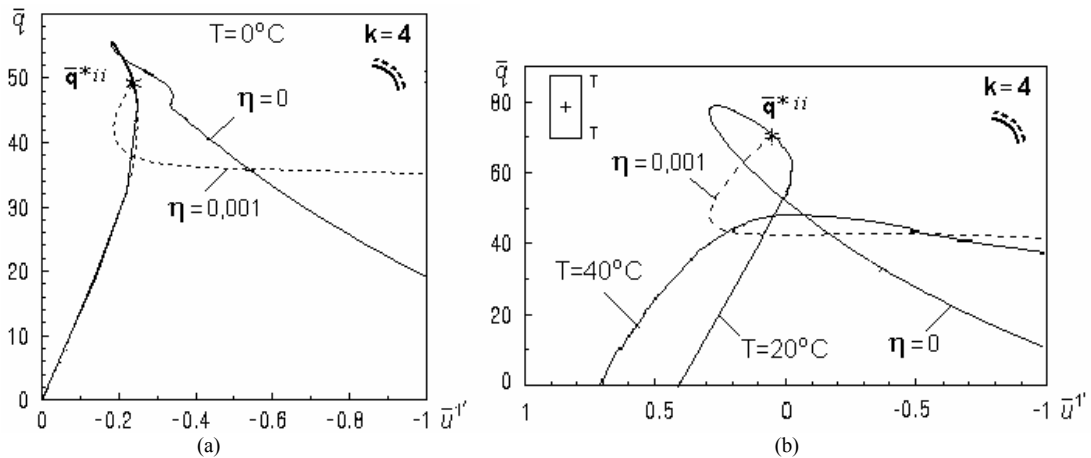
Fig. 14. The $\bar{q} - \bar{u}$ curves of the spherical panel at different levels of preliminary heating

With further heating of the shell ($T = 40°C$), due to the increased effect of the bulging phenomenon and the rise of the panel, the $\bar{q} - \bar{u}$ curves acquire a simpler shape (Fig. 14 (b)). Bifurcation points in the pre-buckling domain are absent.

Such a transformation of the $\bar{q} - \bar{u}$ curves is explained by the influence of heating. Preliminary heating of the panel causes it to bulge in the direction opposite to the applied pressure and increases the rise of the panel (Fig. 15). The more heat then the rise is greater. The initial shape of the panel is shown by a bold dash-dotted line for comparison of the deformation process. Heating the hinged shell to $T = 20°C$ leads to an almost uniform expansion of its volume and an increase in the rise by nearly half of the thickness (Fig. 15 (a)). Buckling of the panel occurs with the formation of an axisymmetric dimple. A more significant preliminary heating of the shell to $T = 40°C$ causes a further increase in the rise of the panel by $0,75h$. Buckling in this case occurs through a snap-through of its central part near the pole (Fig. 15 (b)).

It should be noted that studies presented in [4] have shown that for a panel with a clamped edge, such effects are absent. In this case, the $\bar{q} - \bar{u}$ curves have a simple form, and no bifurcation points are observed in the pre-buckling deformation domain.

Fig. 15. Deformation and buckling modes of the spherical panel, $k=4$

Conclusions

The comprehensive approach developed by the authors for analyzing the behavior of elastic shells under static thermomechanical loads has been applied to study geometrically nonlinear deformation, buckling, and natural vibrations of shells. This work continues the authors' previous research. Special
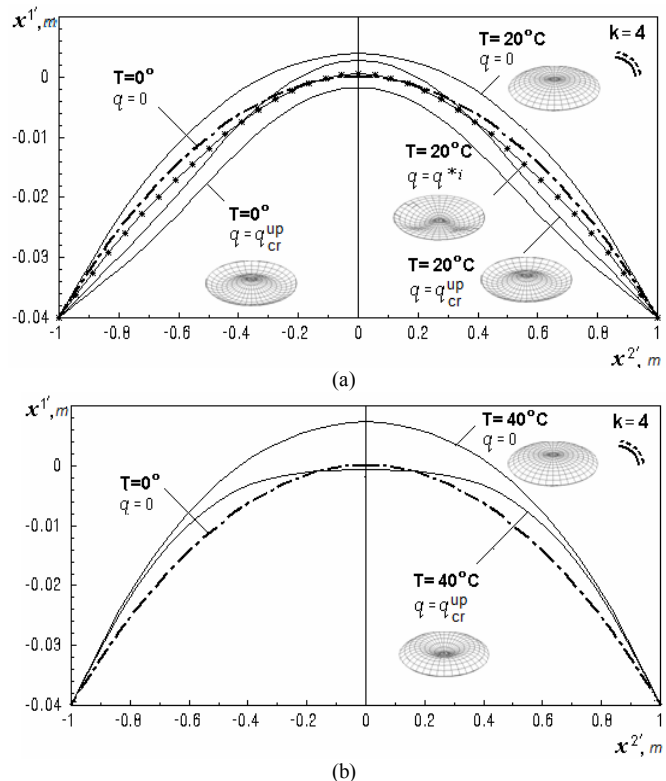
attention is given to shells whose load–deflection curves may exhibit bifurcation points in the pre-buckling domain. The presented numerical examples demonstrate the effectiveness of the method for investigating shell buckling, including the identification of bifurcation points and tracing of branching solution paths.

REFERENCES

1. Bazhenov V.A., Krivenko O.P., Solovei M.O. Nonlinear deformation and stability of elastic shells with inhomogeneous structure (Neliniine deformuvannia ta stiikist pruzhnykh obolonok neodnoridnoi struktury. – K.: ZAT Vipol, 2010. – 316 p. (in Ukrainian).
2. Bazhenov V. A., Krivenko O. P. Stiykist i kolyvannya pruzhnykh neodnoridnykh obolonok pry termosylovykh navantazhennyakh (Buckling and vibrations of elastic inhomogeneous shells under thermomechenical loads)– Kyiv: Karavela Publishing House, 2020. – 187 p. (in Ukrainian).
3. Kryvenko, O.P., Lizunov, P.P., Vorona, Y.V., Kalashnikov, O.B. (2024). Modeling of Nonlinear Deformation, Buckling, and Vibration Processes of Elastic Shells in Inhomogeneous Structure. Int Appl Mech 60 (3) 464- 478. https://doi.org/10.1007/s10778-024-01298-2.
4. Krivenko O.P., Lizunov P.P. Investigation of nonlinear deformation, buckling and natural vibrations of elastic shells under thermomechanical loads using a universal three-dimensional finite element // Strength of Materials and Theory of Structures: Scientific-and-technical collected articles. – Kyiv: KNUBA, 2025. – Issue 114. – P. 93-107.
5. Zenkevich O. Metod konechnykh elementov v tekhnike (Finite element method in engineering). – M.: Mir. – 1975. – 541 p. (in Russian)
6. Sakharov A.S., Kislookiy V.N., Kirichevsky V.V. et al. Metod konechnykh elementov v mekhanike tverdykh tel (Finite element method in solid mechanics) – K.: Vishcha school. Head. publishing house, 1982. – 480 p. (in Russian).
7. Bathe K.-J., Wilson E.L. Numerical methods in finite element analysis, – Prentice-Hall Inc., Englewood Cliffs, N.J., 1976. – 528 p.
8. Reddy J.N. Theory and Analysis of Elastic Plates and Shells, Second Edition – CRC Press, 2006. – 568 p.
9. Oden J. Konechnyye elementy v nelineynoy mekhanike sploshnykh sred (Finite Elements in Nonlinear Continuum Mechanics) . - Moscow: Mir, 1976. - 464 p. (in Russian).
10. Rikards R.B. Metod konechnykh elementov v teorii obolochek i plastin (Finite Element Method in the Theory of Shells and Plates). – Riga: Zinatne, 1988. – 284 p. (in Russian).
11. Lukianchenko O., Kostina O. The Finite Element Metod inProblems of the Thin Shells Theory - LAP LAMBERT Academic Publishing, Beau Bassin, Mauritius, 2019 – 134 p.
12. Karpilovsky V.S. Metod konechnykh elementov i zadachi teorii uprugosti (Finite element method and problems of elasticity theory). – Kyiv: "Sofia A", 2022. - 275 p. (in Russian).
13. Novozhilov V.V. Teoriya tonkikh obolochek (Theory of thin shells). – L.: Sudpromgiz, 1962. - 432 p. (in Russian)
14. Goldenweiser A.L. Teoriya uprugikh tonkikh obolochek (Theory of thin elastic shells). – Moscow: Nauka, 1976. - 512 p. (in Russian)
15. Blokh V.I. Teoriya uprugosti (Theory of elasticity). - Kharkov: Kharkiv State University, 1964. 483 p. (in Russian)
16. Novatsky V. Teoriya uprugosti (Theory of elasticity). - Moscow: Mir, 1975. 872 p. (in Russian)/
17. Rabotnov Yu.N. Mekhanika tverdogo deformiruyemogo tela (Mechanics of a solid deformable body). – Moscow: Nauka, 1988. - 712 p. (in Russian).
18. Kislookiy V.N., Sakharov A.S., Solovey N.A. Momentnaya skhema metoda konechnykh elementov v geometricheski nelineynykh zadachakh prochnosti i ustoychivosti obolochek (Moment scheme of the finite element method in geometrically nonlinear problems of strength and stability of shells). - Strength of Materials, 1977. - No. 7. - Pp. 25–32. (in Russian)
19. Bazhenov V.A., Solovei N.A. Nonlinear Deformation and Buckling of Elastic Inhomogeneous Shells under Thermomechanical Loads. International Applied Mechanics. 2009. Vol. 45, No 9. P 923–953.
20. Bazhenov V.A., Tsikhanovsky V.K., Kislookiy V.M. Metod konechnykh elementov v zadachakh nelineynogo deformirovaniya tonkikh i myagkikh obolochek (Finite element method in problems of nonlinear deformation of thin and soft shells). – Kyiv: KNUBA, 2000. – 386 p.
21. Valishvili N.V. Metody rascheta obolochek vrashcheniya na ETSVM (Methods for calculating shells of revolution on a digital computer). - M.: Mashinostroenie, 1976. - 278 p. (in Russian)
22. Poterya ustoychivosti i vypuchivaniye konstruktsiy: teoriya i praktika / Pod red. Dzh. Tompsona i Dzh. Khanta (Loss of stability and buckling of structures: theory and practice / Ed. J. Thompson and J. Hunt). - M.: Nauka, 1991. - 424 p. (in Russian)
23. Volmir A.S. Ustoychivost' deformiruyemykh sistem (Stability of deformable systems). - M.: Nauka, 1967. - 984 p. (in Russian)
24. Strelets–Streletsky E.B., Zhuravlev A.V., Vodopyanov R.Yu. LIRA–SAPR. Book I. Fundamentals (LIRA–SAPR. Kniga I. Osnovy)/ edited by Dr. of Engineering, Prof. Gorodetsky A.S. - Kiev: LIRALAND, 2019. – 154 p. (in Russian).
25. Karpilovsky V.S., Kriksunov E.Z., Maliarenko A.A., et al. SCAD Office. Version 21. Computing complex SCAD++ (SCAD Office. Versiya 21. Vychislitel'nyy kompleks SCAD++). - Kyiv: SCAD SOFT, 2015. - 848 p. (in Russian).

Кривенко О.П., Лізунов П.П., Калашніков О.Б.

АНАЛІЗ СТІЙКОСТІ ПРУЖНИХ ОБОЛОНОК СТУПІНЧАСТО-ЗМІННОЇ ТОВЩИНИ ПРИ СТАТИЧНИХ ТЕРМОМЕХАНІЧНИХ ВПЛИВАХ

Надано результати комплексного аналізу поведінки пружних оболонок при статичній дії термомеханічних навантажень. Вивчаються процеси геометрично нелінійного деформування, втрати стійкості та власних коливань оболонок. В роботі головна увага приділена визначенню наявності точок розгалуження у докритичній області деформування оболонок. Комплексний метод дослідження поведінки оболонки реалізований як двоетапний алгоритм. На кожному кроці термомеханічного навантаження він поєднує розв'язання статичної задачі геометрично нелінійного деформування оболонки та проведення модального аналізу на цьому кроці. Такий підхід дозволяє визначати критичні стани оболонки як за статичним критерієм (точка максимуму кривої навантаження-прогин), так і за динамічним (навантаження, для якого найнижча частота власних коливань оболонки дорівнює нулю). Метод побудований на основі геометрично нелінійної теорії термопружності, моментної схеми скінченних елементів та універсального тривимірного скінченного елемента. Для визначення точок розгалуження (біфуркації) у докритичній області деформування застосовується методика щодо внесення у вихідну форму оболонки малих несиметричних збурень. Такий підхід забезпечує можливість виходу на нові гілки розв'язку, що відповідають суміжним формам втрати стійкості. Наведені чисельні приклади підтверджують достовірність, універсальність та ефективність методу.

Ключові слова: тонка оболонка, геометрично нелінійне деформування, стійкість, термомеханічне навантаження, біфуркація, універсальний тривимірний скінченний елемент, моментна схема скінченних елементів.

Krivenko O.P., Lizunov P.P., Kalashnikov O.B.

BUCKLING ANALYSIS OF ELASTIC THIN SHELLS WITH STEPWISE VARIABLE THICKNESS UNDER STATIC THERMOMECHANICAL EFFECTS

The results of a comprehensive analysis of elastic shell behavior under static thermomechanical loads are presented. The study focuses on geometrically nonlinear deformation, buckling, and natural vibrations of shells. Special attention is given to the identification of bifurcation points in the pre-buckling domain of shell deformation.The proposed comprehensive method is implemented as a two-stage algorithm. At each step of the thermomechanical loading, it combines the solution of the geometrically nonlinear static problem for the shell with a modal analysis at the same step. This approach allows the determination of critical states according to both the static criterion (maximum point of the load–deflection curve) and the dynamic criterion (load at which the lowest natural frequency of the shell becomes zero). The method is based on the geometrically nonlinear theory of thermoelasticity, the moment scheme of finite elements, and a universal three-dimensional finite element. We apply the methodology of introducing small non-symmetric perturbations into the initial geometry of the midsurface of the shell to determine bifurcation points iin the pre-buckling domain. This approach enables tracing new solution branches corresponding to adjacent forms of buckling. The presented numerical examples confirm the accuracy, universality, and effectiveness of the proposed method.

Keywords: thin shell, geometrically nonlinear deformation, buckling, thermomechanical loading, bifurcation, universal 3D finite element, finite element moment scheme.

Автор (науковий ступінь, вчене звання, посада): кандидат технічних наук, старший науковий співробітник, провідний науковий співробітник НДІ будівельної механіки Київського національного університету будівництва і архітектури, КРИВЕНКО Ольга Петрівна
Адреса: 03037, Україна, м. Київ, проспект Повітряних Сил, 31, КНУБА, НДІ будівельної механіки
Тел.: +38(044) 245-48-29
E-mail: olakop@ukr.net
ORCID ID: https://orcid.org/0000-0002-1623-9679

Автор (науковий ступінь, вчене звання, посада): доктор технічних наук, професор, завідувач кафедри будівельної механіки Київського національного університету будівництва і архітектури ЛІЗУНОВ Петро Петрович
Адреса: 03037, Україна, м. Київ, проспект Повітряних Сил, 31, КНУБА, кафедра будівельної механіки
E-mail: lizunov@knuba.edu.ua
ORCID ID: https://orcid.org/0000-0003-2924-3025

Автор (науковий ступінь, вчене звання, посада): кандидат технічних наук, старший науковий співробітник Державного науково-технічного центру ядерної та радіаційної безпеки, КАЛАШНІКОВ Олександр Борисович
Адреса: 03142, Україна, м. Київ, вул. Василя Стуса, 35-37, Державний науково-технічний центр ядерної та радіаційної безпеки
E-mail: kalash2d@gmail.com
ORCID ID: https://orcid.org/0009-0009-7825-9809